

Electronic structure of FeCr_2S_4 : Evidence of Coulomb enhanced spin-orbit splitting

Soumyajit Sarkar,¹ Molly De Raychaudhury,² I. Dasgupta,³ and T. Saha-Dasgupta^{1,*}

¹*S.N. Bose National Centre for Basic Sciences, Kolkata 700 098, India*

²*Department of Physics, West Bengal State University, Barasat, Kolkata 700 126, India*

³*Department of Solid State Physics, Indian Association for the Cultivation of Science, Kolkata 700 032, India*

(Received 2 September 2009; revised manuscript received 4 October 2009; published 9 November 2009)

The electronic structure of the spinel compound, FeCr_2S_4 , is studied using density-functional-theory-based calculations. Our calculations provide a microscopic understanding of the origin of the insulating behavior of this compound, which turn out to be driven by Coulomb enhanced spin-orbit coupling operative within the $\text{Fe-}d$ manifold. We also investigate the possible role of the structural distortions and compare the calculated optical property data with that of the experimental one.

DOI: 10.1103/PhysRevB.80.201101

PACS number(s): 71.20.Be, 78.20.-e

Transition-metal-based spinel compounds, with general formula AB_2X_4 , are a subject of intense experimental and theoretical activities.¹ FeCr_2S_4 , a member of this family, has attracted attention since early '70s. The interest in FeCr_2S_4 is regained due to the recent discovery of large negative magnetoresistance (MR).² The MR effect has been discussed in the context of nondouble exchange-like model because of the absence of mixed valency and lack of any strong evidence of formation of Jahn-Teller (JT) polarons.³ The physical properties of this compound are rather intriguing. The system is insulating above the magnetic transition temperature ~ 180 K, signaled by the disappearance of the ferrimagnetic coupling between Fe^{2+} and Cr^{3+} ions and also below 150 K where the magnetic order persists, while in the intermediate range (150–180 K) it is metallic.^{2,3} Though there have been several experimental studies on this compound, the activities on theoretical front have been minimal, except for the initial calculation⁴ by Park *et al.*

In this Rapid Communication, we report a detailed density-functional theory (DFT) study of the electronic structure of this material. Our study sheds light on the microscopic mechanism of the insulating solution at the low-temperature phase, unraveling the role of Coulomb-enhanced spin-orbit (SO) coupling. We also discuss the possible role of the structural distortion and compare the calculated reflectivity spectrum with that of the measured data. The calculations have been carried out within the frame work of linear augmented plane-wave (LAPW) basis with no shape approximation to the potential and charge density as implemented in WIEN2K code.⁵ The number of plane waves is restricted using the criteria muffin-tin radius multiplied by k_{max} yielding a value of 7. The total Brillouin zone (BZ) was sampled with 256 k points for self consistent calculations and 404 k points for optical calculations.

Figure 1 shows spin-polarized density of states of FeCr_2S_4 , considering the experimentally measured cubic $Fd\bar{3}m$ space group with crystal structure parameters as $a=9.99$ Å and $u_s=0.384$.^{4,6} The calculation has been carried out with the generalized gradient approximation (GGA) by Perdew, Bruke, and Ernzerhof⁷ for exchange-correlation functional. The deviation of S position from the ideal value of 0.375 introduces trigonal distortion at CrS_6 octahedra in terms of two distinct S-S bond lengths of 3.28 and 3.54 Å.

The FeS_4 tetrahedron unit in the $Fd\bar{3}m$ space group on the other hand is ideal. The octahedral crystal-field surrounding Cr atom splits the Cr- d levels into low-lying t_{2g} and high-lying e_g blocks with some mixing between the two due to nonzero trigonal distortion, while the tetrahedral crystal-field surrounding Fe atom splits the Fe- d levels in low-lying e and high-lying t_2 blocks. The Cr d levels are unoccupied in down-spin channel with Cr t_{2g} states occupied in up-spin channel. The Fe d levels are completely occupied in down-spin channel with partially filled e block in up-spin channel. This confirms the nominal 3+ and 2+ valency of Cr and Fe, respectively. The superexchange interaction between half-filled Cr t_{2g} states and half-filled Fe d states gives rise to antiferromagnetic coupling between Cr and Fe, while the superexchange interaction between empty Cr e_g states and partially filled Fe levels gives rise to ferromagnetic coupling between Cr and Fe. The former wins giving rise to net antiferromagnetic coupling between Cr and Fe with magnetic moments at Cr and Fe sites 2.75 and $-3.14\mu_B$, respectively, and a total magnetic moment of $2\mu_B/\text{f.u.}$ The energy levels of Fe and Cr, taking into account the S covalency, are shown in the right panel of Fig. 1. The crystal-field splitting at the Fe site is found to be smaller than the spin splitting, while at the Cr site they are found to be comparable. Energetically the

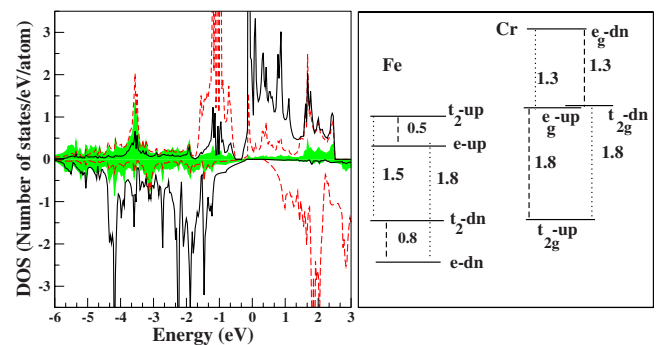


FIG. 1. (Color online) Left panel: spin-polarized partial density of states calculated within GGA. Fe- d states, Cr- d states, and S- p states are presented by solid black lines, broken gray (red) lines and filled light gray (green) areas, respectively. Energy is plotted with respect to Fermi energy (E_f). Right panel: the energy levels of Fe and Cr d levels in eV unit.

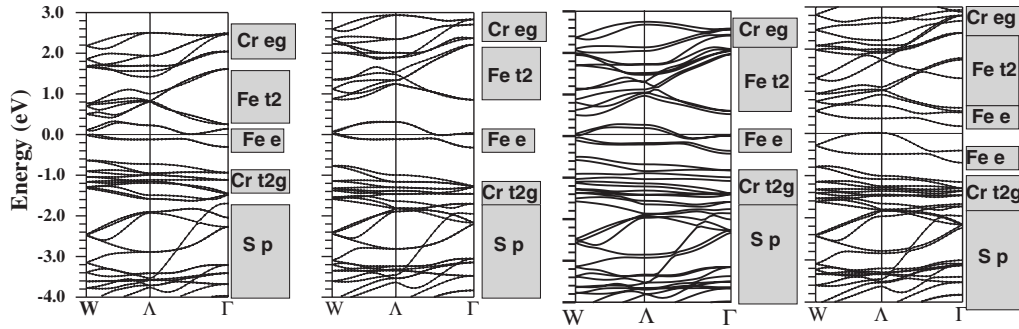


FIG. 2. Band structure in the up-spin channel. Energies are plotted with respect to E_F in eV unit. From left to right: band structures calculated with GGA, GGA+ U , GGA+SO, and GGA+ U +SO, respectively. In the GGA+ U , and GGA+ U +SO calculations, the U values were chosen as $U_{Fe}=2.50$ eV, $U_{Cr}=1.50$ eV, and $J_{Fe}=0.9$ eV, $J_{Cr}=0.8$ eV.

Cr e_g -up-spin states are close to Fe d states in the up-spin channel. This causes significant hybridization between empty Cr e_g and Fe d states in the up-spin channel, as has been pointed out by Brossard *et al.*⁸ Since the Fe e states in the up-spin channel are partially filled with one electron and all the other states are either completely empty or filled, GGA leads to half-metallic solution in contrast to the insulating solution, as observed experimentally. Both, missing correlation effect⁴ as well as the JT effect,⁹ have been discussed in literature to account for this discrepancy. In connection to the JT effect, it should be remembered that the relevant JT ion Fe²⁺ is in tetrahedral environment with Fe e states being the relevant degree of freedom. The JT distortion within the e manifold which point in between the S ions is expected to be weak. Furthermore the distortion at A sublattice of a AB_2X_4 spinel which is a diamond sublattice is found to be much weaker than B sublattice in general. Recently the role of JT distortion in the context of spinels in general has been questioned.¹ For FeCr₂S₄, though there are indications of some structural distortions at low temperature (≤ 60 K),^{9,10} the nature and existence of this distortion are debated. The x-ray and neutron-diffraction studies⁶ concluded that the sample remains in $Fd\bar{3}m$ symmetry down to a temperature of 4.2 K. However, a recent transmission electron microscopic studies,¹¹ assigned a noncentrosymmetric $F\bar{4}3m$ space group to the low-temperature structure. It is to be noted that although the reduction in symmetry from $Fd\bar{3}m$ to $F\bar{4}3m$ would give rise to two inequivalent Fe ions in the unit cell, it will fail to lift the degeneracies within the e block avoiding the JT distortion. We will return to this point later.

Leaving aside the possible role of structural distortion, we first studied the electronic structure of FeCr₂S₄ in $Fd\bar{3}m$ symmetry considering the influence of various interactions, as summarized in Fig. 2. The band dispersions of FeCr₂S₄ along the high-symmetry points of the BZ of the cubic-face-centered (FCC) lattice in the up-spin channel are shown in Fig. 2. The band structures of the corresponding down-spin channel, which have either completely occupied or empty bands, are not shown. From left to right, the various panels show the results obtained on the basis of GGA, GGA+ U , GGA+SO, and GGA+ U +SO calculations. The GGA band structure, which corresponds to the DOS shown in Fig. 1, exhibits degenerate Fe e bands crossing E_f making the sys-

tem metallic. The e bands correspond to the orbitals of symmetry $3y^2-r^2$ and z^2-x^2 in the global frame of reference. Upon switching on the missing correlation in GGA, in the form of GGA+ U calculation as shown in the second panel of Fig. 2, we find the solution still remains metallic with degenerate e bands crossing the Fermi level. The GGA+ U method which is designed to make the configurations with larger magnetization more favorable is not effective here in a manifold of degenerate bands involving only one spin channel, though the double-counting correction remains operative. As a result, the addition of onsite U enhances the gap between e and t_2 blocks of Fe d states compared to GGA results which is found to increase with increasing value of U , keeping the structure of degenerate e bands crossing the Fermi level intact. The inclusion of Hubbard U is therefore not effective in driving the insulating solution, contrary to previous statements in the literature.^{4,12} The third panel shows the results by inclusion of the spin-orbit coupling. The orbital moments at Cr and Fe sites are found to be $-0.02\mu_B$ and $-0.08\mu_B$, respectively, with orbital moment pointing opposite to the spin moment for Cr and along for Fe (see Table I). The spin and orbital moments have the same sign for Fe, but opposite sign for Cr, due to the fact that the d states of Fe²⁺ are more than half filled, but those of Cr³⁺ are less than half filled.

The orbital moment at the Cr site is found to be small due to the d^3 configuration of Cr. The orbital moment at Fe site however is large which is surprising since the spin-orbit interaction (SOI) within e levels of Fe comprising of orbital states that differ by two units of angular momentum ($l_z=0, \pm 2$) should vanish. This however can happen through coupling with empty Fe t_2 orbitals. In order to understand the role of SOI in the Fe d manifold, we considered the Hamiltonian¹³ given by

TABLE I. Magnetic moments of Fe and Cr ions in μ_B .

	Fe		Cr	
	Orbital moment	Spin moment	Orbital moment	Spin moment
GGA		-3.135		2.750
GGA+ U		-3.279		2.720
GGA+SO	-0.077	-3.133	-0.024	2.754
GGA+ U +SO	-0.134	-3.270	-0.026	2.690

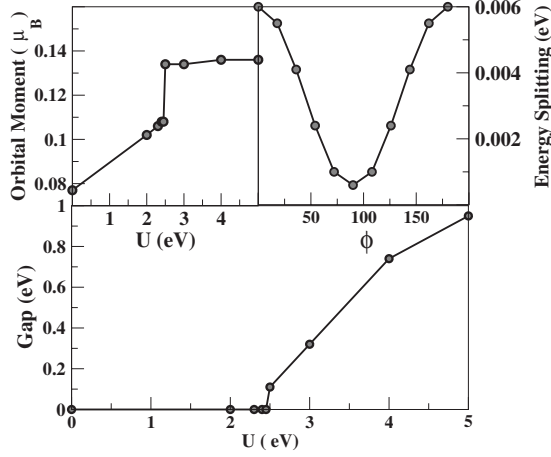


FIG. 3. Upper panel: variation in Fe orbital moment plotted as function of U applied on Fe site (left panel) and the splitting between Fe z^2-x^2 and $3y^2-r^2$ levels in eV plotted as function of angle ϕ (right panel, see text for details). Lower panel: variation in band gap with U value applied on Fe site.

$$\hat{H}_{SO} = \lambda \hat{S}_z \left(\hat{L}_z \cos(\theta) + \frac{1}{2} \hat{L}_+ \exp^{-i\phi} \sin \theta + \frac{1}{2} \hat{L}_- \exp^{i\phi} \sin \theta \right)$$

where θ and ϕ are the zenith and azimuthal angles of the magnetization direction of the spin moment. We have neglected the coupling between the up and down-spin states due to SOI as they are energetically separated by 1.5–2 eV. Expressing the angular parts of the d orbitals in terms of the spherical harmonics, we find that the SOI introduces coupling between the empty Fe $|yz\rangle$, $|xz\rangle$ states and $|z^2-x^2\rangle$, $|3y^2-r^2\rangle$ states. The coupling $\langle yz | H_{SO} | z^2-x^2 \rangle$ is $\propto \sin \theta \cos \phi$, $\langle xz | H_{SO} | z^2-x^2 \rangle$ is $\propto \sin \theta \sin \phi$, and similar dependences are found for the coupling with $|3y^2-r^2\rangle$ state. This points to the fact that the coupling and, consequently, the SOI-induced splitting between Fe $3y^2-r^2$ and z^2-x^2 states are strongest for $\theta = \frac{\pi}{2}$, i.e., when the spin-quantization axes is in the xy plane. Considering the onsite energies of Fe d orbitals as shown in the right panel of Fig. 1 and a typical value of spin-orbit coupling parameter $\lambda = -0.02$ eV, the splitting between Fe $3y^2-r^2$ and z^2-x^2 as a function of varying ϕ with fixed value of $\theta = \frac{\pi}{2}$ is shown in the upper right panel of Fig. 3. This shows the splitting to be strongest for $\phi=0$.

This splitting however is not enough to make the system insulating. The situation changes remarkably upon application of GGA+ U +SO, as is shown in the last panel of Fig. 2. This exhibits clear evidence of Coulomb enhanced spin-orbit splitting as has been recently shown for Sr_2RhO_4 (Ref. 14) and for double perovskite $\text{Ba}_2\text{NaOsO}_6$.¹³ For choices of $U_{\text{Fe}}=2.50$ eV, $U_{\text{Cr}}=1.50$ eV, $J_{\text{Fe}}=0.9$ eV, and $J_{\text{Cr}}=0.8$ eV, the orbital moment at Fe site is found to be renormalized to $0.13\mu_B$ and the spin-orbit splitting between Fe $3y^2-r^2$ and z^2-x^2 opens up a gap of 0.1 eV with z^2-x^2 completely occupied and $3y^2-r^2$ being completely empty. This leads to antiferro-orbital ordering driven by Coulomb-enhanced spin-orbit coupling. The size of the gap increases with the increase of U at Fe site since double-counting correction

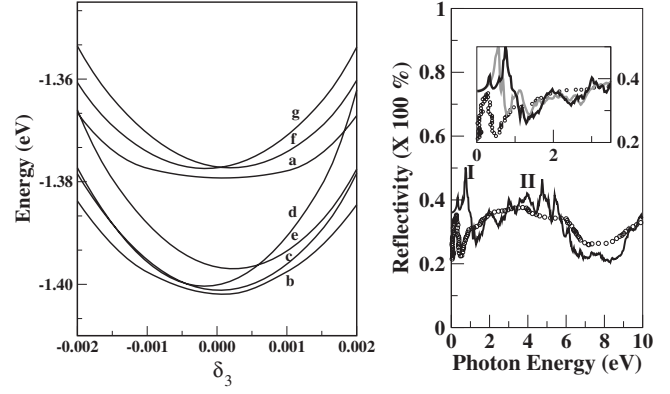


FIG. 4. Left panel: a series of minimum-energy curves plotted against the variation of Cr position (δ_3), for various choices of S movements: (a) $\delta_1 = \delta_2 = 0.0090$; (b) $\delta_1 = 0.0095$ $\delta_2 = 0.0085$; (c) $\delta_1 = 0.0085$ $\delta_2 = 0.0095$; (d) $\delta_1 = 0.0085$ $\delta_2 = 0.0100$; (e) $\delta_1 = 0.0100$ $\delta_2 = 0.0085$; (f) $\delta_1 = 0.0090$ $\delta_2 = 0.0095$; (g) $\delta_1 = 0.0095$ $\delta_2 = 0.0090$. Right panel: comparison of calculated reflectivity spectrum within GGA+ U +SO (solid line) and measured spectrum (Ref. 18) (dotted line). Two calculated spectra in the inset, shown as black and gray solid lines, correspond to calculations in undistorted and distorted crystal structure, respectively.

pushes the empty local states further apart, the orbital moment however saturates. Figure 3 shows the variation in the band gap and Fe orbital moment as a function of U . The magnetocrystalline anisotropy was found to be 10 meV/Fe obtained by taking the energy difference between calculations with the spin quantization along $[001]$ and $[110]$, the spin quantization being favored for $[110]$. The spin quantization is found to be further favored along $[100]$ by 20 meV/Fe compared to $[110]$, consistent with our findings from Fe t_2 mediated SOI.

In the next step, to check the possibility of S and Cr movements in the low-temperature crystal structure, as suggested in Ref. 11, we carried out total-energy calculations within the framework of GGA+ U +SO with same choice of U , J values as in Fig. 2, assuming the $F\bar{4}3m$ symmetry. The $F\bar{4}3m$ space group gives rise to two inequivalent S and Fe ions and single inequivalent Cr ion. The inequivalent ionic positions of Cr, Fe1, Fe2, S1 and S2 in $F\bar{4}3m$ can be written as (x_3, x_3, x_3) with $x_3 = 0.625 + \delta_3$, $(0, 0, 0)$, $(\frac{1}{4}, \frac{1}{4}, \frac{1}{4})$, (x_1, x_1, x_1) with $x_1 = 0.375 + \delta_1$ and (x_2, x_2, x_2) with $x_2 = 0.875 - \delta_2$, respectively. Setting $\delta_1 = \delta_2$ and $\delta_3 = 0.0$ in the above, one recovers the $Fd\bar{3}m$ space group.¹⁵ (δ_1, δ_2) governs the distortion related to S movement, while δ_3 governs the trigonal movement of Cr along the $[111]$ direction. The total-energy curve as shown in left panel of Fig. 4 shows a tendency of small Cr movement as well as some movements of S. These S movements create two inequivalent FeS_4 tetrahedra with two different volumes rather than causing distortion of the individual tetrahedra. Repeating electronic structure calculations with ionic positions as given in $F\bar{4}3m$ crystal structure shows that S movements tend to reduce the band gap, while the Cr movement tends to increase it. The optimized values of S and Cr movements, given by curve “b,” gave rise to a gap of 0.2 eV.

Finally there have been reports of optical reflectivity and conductivity¹⁶⁻¹⁸ measurements on FeCr_2S_4 . We therefore considered it worthwhile to compute the optical properties and compare with experimentally measured data. For this purpose, the reflectivity spectrum was calculated using the joint density of states and the dipole matrix elements.¹⁹ The right panel of Fig. 4 compares the calculated and experimental¹⁸ reflectivity spectrum. Though the experimental spectra were measured at room temperature, such a comparison is found to be reasonable. None of the optical experiments reported to date show any substantial modification of the optical spectrum in the energy region explored as temperature is changed,¹⁷ which indicates that the gross electronic structure remains unaltered by the temperature variation. The experimental spectrum shown as dotted line in right panel of Fig. 4 shows a peaked structure (structure I) at about 0.3 eV and a broad one (structure II) between 0.7 and 7.0 eV. In between these two structures there is a dip at about 0.5 eV.²⁰ The reflectivity data calculated within GGA+ U +SO, as shown in solid lines in right panel of Fig. 4, show in general good agreement with experimental data. The broad shape and position of structure II, which originates from the transitions involving fully occupied Cr t_{2g} and S p states in the valence band, and the empty Fe d and Cr e_g and S p hybridized states in the majority-spin channel and the fully filled Fe d hybridized with S p states to the empty Cr d states in the minority-spin channels, agrees very well with the experimental one. Structure I in the calculated spectrum, starts from 0.25 eV and ends at 1.25 eV. This structure is due to a transition among the SO-split majority Fe- e spins. Transitions among the Fe d - d states are allowed due to loss of inversion symmetry at the Fe site.¹⁷ Although the starting point agrees well with the experimental value, the peak is

much broader in the calculation. While there can be several different reasons for this discrepancy,²¹ an important issue to consider is the influence of the structural distortion. The inset in the right panel of Fig. 4 shows the change in the reflectivity caused by the movements of Cr and S (spectrum shown in solid gray line in the figure). It is found to alter structure I while keeping all the structures beyond 1.2 eV unaltered. Structure I narrows down and moves down in energy and the following dip moves down, thereby providing a better agreement in the low energy feature. The precise determination of the ionic positions therefore seems crucial.

In conclusion, using first-principles DFT calculations we have explored the origin of insulating behavior of FeCr_2S_4 in the low-temperature regime. Our study shows that the insulating behavior is driven by spin-orbit coupling within Fe e states which gets renormalized in presence of Coulomb correlation. This adds FeCr_2S_4 in the list of compounds exhibiting Coulomb enhanced SOI.^{13,14} The unexpectedly large spin-orbit coupling within Fe e states is found to be mediated by coupling with empty Fe t_2 states. We also explored the possible role of low-temperature structural distortion as has been discussed in the literature. Our total-energy calculation shows tendency of both S and Cr movements. Comparison of calculated reflectivity spectrum with experimentally measured data shows improved agreement in the mid infrared regime upon inclusion of structural distortion. More experimental studies are needed for a complete understanding of the optical properties.

S.S. thanks CSIR for financial support. M.D.R. acknowledges computing support from SNBose Centre. T.S.D. acknowledges funding through Swarnajayanti grant and Advanced Materials Research Unit.

*Corresponding author; tanusri@bose.res.in

¹P. G. Radaelli, *New J. Phys.* **7**, 53 (2005).

²A. P. Ramirez, R. J. Cava, and J. Krajewski, *Nature (London)* **386**, 156 (1997).

³Z. Chen, S. Tan, Z. Yang, and Y. Zhang, *Phys. Rev. B* **59**, 11172 (1999).

⁴M. S. Park, S. K. Kwon, S. J. Youn, and B. I. Min, *Phys. Rev. B* **59**, 10018 (1999).

⁵Full-potential LAPW (P. Blaha, K. Schwartz, G. K. H. Madsen, D. Kvasnicka, and J. Luitz, WIEN2K).

⁶G. Shirane, D. E. Cox, and S. J. Pickard, *J. Appl. Phys.* **35**, 954 (1964).

⁷J. P. Perdew, K. Burke, and M. Ernzerhof, *Phys. Rev. Lett.* **77**, 3865 (1996).

⁸L. Brossard, J. L. Dormann, L. Goldstein, P. Gibart, and P. Renaudin, *Phys. Rev. B* **20**, 2933 (1979).

⁹M. R. Spender and A. H. Morrish, *Solid State Commun.* **11**, 1417 (1972).

¹⁰M. Eibschutz, S. Shtrikman, and Y. Tenenbaum, *Phys. Lett. A* **24**, 563 (1967).

¹¹M. Mertinat, V. Tsurkan, D. Samusi, R. Tidecks, and F. Haider, *Phys. Rev. B* **71**, 100408(R) (2005).

¹²V. Fritsch *et al.*, *Phys. Rev. B* **67**, 144419 (2003).

¹³H. J. Xiang and M.-H. Whangbo, *Phys. Rev. B* **75**, 052407 (2007).

¹⁴G. Q. Liu, V. N. Antonov, O. Jepsen, and O. K. Andersen, *Phys. Rev. Lett.* **101**, 026408 (2008).

¹⁵P. R. Staszak, J. E. Poetzinger, and G. P. Wirtz, *J. Phys. C: Solid State Phys.* **17**, 4751 (1984).

¹⁶T. Ogasawara *et al.*, *J. Phys. Soc. Jpn.* **75**, 083707 (2006).

¹⁷K. Ohgushi, T. Ogasawara, Y. Okimoto, S. Miyasaka, and Y. Tokura, *Phys. Rev. B* **72**, 155114 (2005).

¹⁸K. Ohgushi *et al.*, *J. Phys. Soc. Jpn.* **77**, 034713 (2008).

¹⁹S. Saha, M. De Raychaudhury, and T. Saha-Dasgupta, *Phys. Rev. B* **77**, 155428 (2008).

²⁰Interestingly the spectrum shows an *upturn* below structure I (not shown in the figure), which is certainly not expected in the room-temperature insulator regime. Further experiments in the far-infrared region are necessary to resolve this matter.

²¹P. Puschnig and C. Ambrosch-Draxl, *Phys. Rev. B* **66**, 165105 (2002); D. I. Bilc, R. Orlando, R. Shaltaf, G. M. Rignanese, J. Iniguez, and P. Ghosez, *ibid.* **77**, 165107 (2008); N. Marom *et al.*, *J. Chem. Phys.* **128**, 164107 (2008); S. Suhai, *Int. J. Quantum Chem.* **29**, 469 (2004).